RESEARCH ARTICLE
doi: 10.2306/scienceasia1513-1874.2026.054

ScienceAsia 52 (3): 2026: ID 2026054: **1–8**

Development and characterization of the PVA/PVP: MO composite films for lead-free X-ray shielding applications

Paitoon Boonsong[a], **Chulalak Damphathik**[b], **Anucha Watcharapasorn**[c,d], **Ampika Rachakom**[e,*]

[a] Regional Medical Sciences Center 1 Chiang Mai, Department of Medical Sciences, Chiang Mai 50180 Thailand
[b] Regional Medical Sciences Center 2 Phitsanulok, Department of Medical Sciences, Phitsanulok 65000 Thailand
[c] Department of Physics and Materials Science, Faculty of Science, Chiang Mai University, Chiang Mai 50200 Thailand
[d] Center of Excellence in Materials Science and Technology, Materials Science Research Center, Faculty of Science, Chiang Mai University, Chiang Mai 50200 Thailand
[e] Division of Science, Faculty of Science and Agricultural Technology, Rajamangala University of Technology Lanna, Chiang Mai 50300 Thailand

*Corresponding author, e-mail: ampika_aom@rmutl.ac.th

Received 23 Apr 2025, Accepted 20 May 2026
Available online 14 Jun 2026

ABSTRACT: Amid growing concerns over the environmental and health hazards linked to lead-based X-ray shielding materials, this study examines the development of polyvinyl alcohol/polyvinylpyrrolidone (PVA/PVP) blend films containing 50 wt% metal oxides (MOs) such as Bi_2O_3, WO_3, Ta_2O_5, MoO_3, and $BaTiO_3$. The films were synthesized via the solution casting method to assess their suitability as alternative materials for X-ray shielding. The X-ray transmission factor (TF), linear attenuation coefficient (LAC), half-value length (HVL), and tenth-value layer (TVL) were evaluated at different X-ray energies. Theoretical values of the mass attenuation coefficients (MAC_{xcom}) were also determined using the XCOM software. Compared to the other samples, the PVA/PVP blend film containing 50 wt% Bi_2O_3 (PPB) demonstrated the highest X-ray attenuation efficiency, with a TF value of 2.87% at 28 kV_p and 47.99% at 80 kV_p. The LAC values for the PPB sample were measured as 72.28, 27.80, 17.17, and 14.94 cm^{-1} at 28, 61, 70, and 80 kV_p, respectively. The PVA/PVP/Bi_2O_3 composite exhibited the lowest HVL and TVL values, signifying its superior shielding efficiency. Additionally, the XCOM data confirmed that the incorporation of metal oxides significantly enhanced the MAC_{xcom} values, particularly at the K, L, and M absorption edges, thereby improving energy absorption and attenuation. The PVA/PVP blend film loaded with 50 wt% Bi_2O_3 are promising candidates for lead-free X-ray shielding materials, aligning with the increasing demand for more sustainable and non-toxic radiation protection in medical applications.

KEYWORDS: polyvinyl alcohol, polyvinylpyrrolidone, lead-free X-ray shielding materials, blend film, composite film

INTRODUCTION

X-rays with energy levels between 20 and 125 keV have demonstrated remarkable applications in medical imaging, including mammography, dental imaging, and general radiology [1]. These energy levels are carefully selected to optimize image quality while minimizing patient radiation exposure. For example, in mammography, a typical X-ray tube operates within a voltage range of 25 to 28 kV_p to capture standard breast images, with the mean X-ray energy at 28 kV_p being approximately 20 keV [2]. Tube voltages between 60 and 70 kV_p are commonly used for intraoral X-ray examinations, with the mean energy at 60 kV_p ranging from 34 to 39 keV [3–5]. For diagnostic radiology, tube voltages typically range from 50 to 120 kV_p, with specific recommendations for various body parts. A tube voltage of 70 kV_p is ideal for imaging areas such as the elbow, foot, ankle, leg, knee, forearm, and pediatric extremities, while 80 kV_p is preferred for imaging the abdomen, pelvis, unilateral hip, lumbar spine, pediatric chest, and skull [6]. The mean energy at 70 kV_p is reported to range from 39 to 42 keV, while at 80 kV_p, it ranges between 42 and 46 keV [3–5]. These energy levels are fundamental in ensuring the quality and diagnostic utility of the images produced. However, long-term exposure to X-rays can have detrimental effects on human health, resulting in severe autonomic nerve dysfunction, poor haematopoiesis, lens turbidity, and spermatogenesis disorder [7]. This highlights the importance of radiation protection and the role of shielding materials in minimizing risks associated with X-ray exposure. Radiation-shielding materials are vital for safeguarding patients and healthcare workers from the potentially harmful effects of radiation.

Generally, lead (Pb) has traditionally been the material of choice for radiation shielding due to its excellent attenuation efficiency, ease of processing, and reasonable cost. However, the use of Pb has limitations in applications due to its toxicity and the need for alternative properties such as low cost, flexibility, chemical stability, mechanical strength, and lightweight materials. To overcome these limitations, polymer matrix materials have emerged as a promising alternative for radiation shielding. These materials offer several benefits, including cost-effectiveness, flexibility, chemical

stability, lightweight design, low maintenance, and superior workability. Nevertheless, pure polymers are inadequate for effective shielding due to their low atomic number (Z) characteristics. To address this limitation, numerous studies have focused on the development of polymer composites incorporating high-Z elements as potential substitutes for lead in radiation shielding applications. High-Z elements, such as titanium (Z_{Ti}=22) [8–10], iron (Z_{Fe}=26) [11, 12], molybdenum (Z_{Mo}=42) [13], barium (Z_{Ba}=56) [10, 12], tantalum (Z_{Ta}=73) [14], tungsten (Z_{W}=74) [15–17], and bismuth (Z_{Bi}=83) [18, 19], have shown promise. These high-Z elements, whether employed individually or in combination, serve as substitutes for lead (Z_{Pb}=82) in lead-free radiation-shielding materials, demonstrating significant advancements in X-ray protection.

Polyvinyl alcohol (PVA) and polyvinylpyrrolidone (PVP) are synthetic biopolymers with excellent water solubility, low toxicity, flexibility, good film-forming ability, high abrasion resistance, optical transparency, non-carcinogenicity, biocompatibility, and low cost [17–20]. The blending of these two polymers results in the formation of clear transparent sheets after drying. It has been reported that the hydroxyl group of PVA forms a hydrogen bond with the carbonyl group of PVP, leading to the formation of a miscible solution [17, 18]. The resulting blend exhibits enhanced film-forming ability and improved physical properties. PVA/PVP films combined with Fe_2O_3 [11], WO_3 [17], and Bi_2O_3 [18] have been investigated as alternative materials to lead for radiation shielding applications. These additives enhance the probability of the shield interacting with the incoming photons, increasing the amount of attenuated radiation. The K-edge effect refers to a sharp increase in the X-ray attenuation coefficient. The K-edges of tungsten (W), tantalum (Ta), barium (Ba), and molybdenum (Mo) are reported to be 69.5, 67.4, 37.4, and 20.0 keV [21], respectively. These elements have an excitation photon energy below the K-edge energy of lead (88.0 keV), which lies in the weak absorption region of lead. Additionally, the K-edge of bismuth (90.5 keV) is nearly equal to that of lead [21].

This study aims to develop lead-free X-ray shielding materials by fabricating PVA/PVP composites incorporating 50 wt% of various metal oxides, including Bi_2O_3, WO_3, Ta_2O_5, MoO_3, and $BaTiO_3$, and evaluating their effectiveness in radiation attenuation. The PVA/PVP/MO composites were characterized in terms of TF, LAC, HVL, and TVL. These measurements were set up using a mammographic unit at 28 kV_p, intraoral X-ray machines at 61 kV_p, and a general X-ray machine at both 70 and 80 kV_p. Additionally, the theoretical values of the MAC_{xcom} were calculated using the XCOM program [22, 23] for energy levels ranging from 1 keV to 200 keV. This analysis provided insight into the effectiveness of the composites as radiation-shielding materials, and the findings were discussed in detail.

MATERIALS AND METHODS

Materials

Polyvinyl alcohol (PVA, M_W = 89,000–98,000 g/mol), polyvinylpyrrolidone K 90 (PVP, M_W = 360,000 g/mol), bismuth (III) oxide (Bi_2O_3, 99.9%), tungsten (VI) oxide (WO_3, 99.9%), tantalum (V) oxide (Ta_2O_5, 99%), molybdenum (VI) oxide (MoO_3, 99.9%), and barium titanate (IV) ($BaTiO_3$, 99%) were purchased from Sigma-Aldrich (USA). Deionized water (DI) was obtained from RCI Labscan (Thailand).

Equipment

Analytical balance (And: GR-200, Japan), hotplate stirrer (Ika: Yellow line MAG HS 7, Germany), magnetic stirring bar (Isolab, Germany), cabinet dry (FCDE60, China), ultrasonic bath (Skymen: JP-040S, China), cylinder (50 ml, Isolab), petri dish glass (Numra, Czech), beaker glass (50&100 ml, Duran, Germany) were used for film processing. For X-ray attenuation measurement, radiation meter (RaySafe: X2&R/F Sensor, Sweden), mammographic X-ray machine (Hologic: Selenia Dimensions, USA), intraoral X-ray machine (ASAHI: C610NS, Japan), and general X-ray machine (Shimadzu: RAD Speed Pro, Japan) were used to examine.

Synthesis method

The PVA, PVP, and metal oxides, including Bi_2O_3, WO_3, Ta_2O_5, MoO_3, and $BaTiO_3$, were used to prepare the PVA/PVP: MO blend films via the solution casting technique, as illustrated in Fig. 1. Initially, 25 wt% of PVA, 25 wt% of PVP, and 50 wt% of MO powders were separately dissolved in 20 ml of DI water in a beaker. The solutions were then stirred continuously with a magnetic stirrer on a hot plate at 80 °C for 1 h to prepare each solution. These solutions were subsequently mixed and stirred at 80 °C for 2 h to ensure homogeneity. Finally, the homogeneous solutions were poured into a Petri dish glass with dimensions of 10 cm × 2 cm. Then, the mixtures were ultrasonicated for 30 min to eliminate bubbles and allowed to dry for 3 days in a cabinet at 35 °C with 10% RH. After drying, the samples were carefully removed from the casting plate, stored appropriately, and subsequently prepared for X-ray attenuation measurements. The samples of PVA/PVP, PVA/PVP: Bi_2O_3, PVA/PVP: WO_3, PVA/PVP: Ta_2O_5, PVA/PVP: MoO_3, and PVA/PVP: $BaTiO_3$ were abbreviated as PP, PPB, PPW, PPT, PPM, and PPBT, respectively.

X-ray attenuation measurement

The X-ray shielding properties of the PVA/PVP: MO blend films were measured under various conditions: (a) 28 kV, 50 mAs, (b) 60 kV, 10 mA, 400 ms, and (c) 70 and 80 kV, 100 mA, 100 ms. The distance between the X-ray tube and the detector was set to 66, 100, and 100 cm using mammographic, intraoral, and general

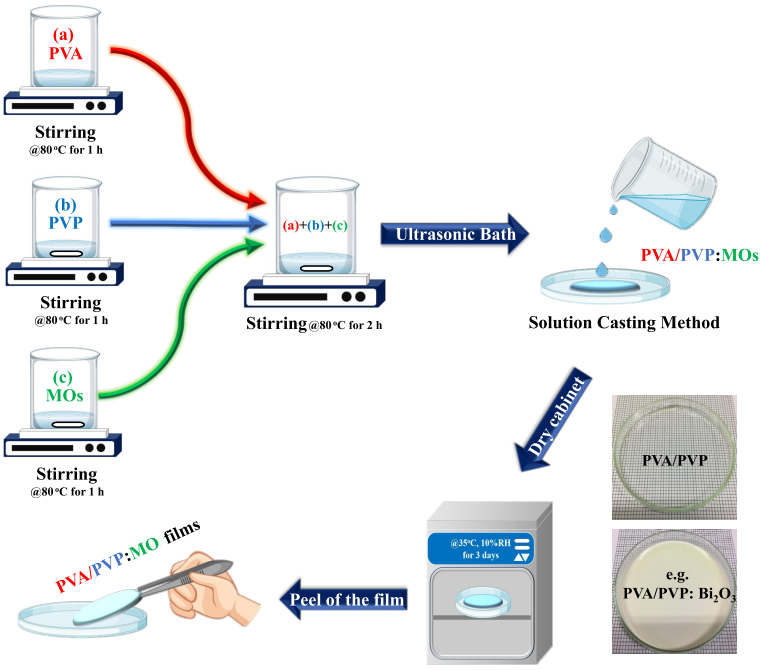

Fig. 1 Schematic diagram of the PVA/PVP: MO blend films prepared by solution casting method.

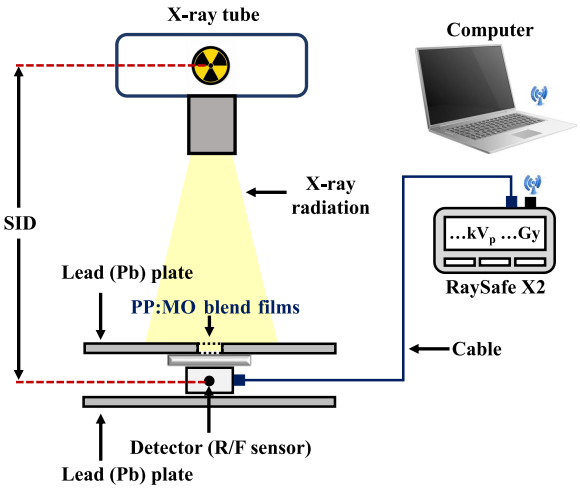

Fig. 2 Schematic diagram of the X-ray transmission technique.

X-ray machines, respectively. The samples were placed between a 4-mm-thick lead blank holder with an area of 2.5×2.5 cm^2, and the detector, the X2 R/F sensor, is capable of measuring tube voltage (kV_p) within the range of 40–150 kV_p, with an uncertainty of ±2%. The system is capable of measuring radiation doses ranging from 1 nGy to 9999 Gy, with an uncertainty of ±5% or ±5 nGy (0.5 μR) at positions in close proximity to the detector as shown in Fig. 2. The experimental setup was arranged in compliance with IEC 61331:1 standard [24].

The TF can be expressed as $TF(\%) = (I/I_0) \times 100\%$. To evaluate the shielding performance of the samples, the TF is a standard method for estimating the specific number of photons that can pass through the attenuator. X-ray attenuation properties of a material are described by the Lambert-Beer law. The relationship between X-rays and matter is given by the following equation: $I/I_0 = e^{-\mu t}$, where I is the intensity of the attenuated beam, I_0 is the initial intensity, t (cm) is the thickness, and the μ is the linear X-ray attenuation coefficient of the materials. The concepts of HVL and TVL are fundamental parameters commonly used to evaluate the effectiveness of shielding materials. The μ was used to determine the HVL using the following equation: $HVL = 0.693/\mu$. The HVL was employed to determine the sample thickness required to attenuate the X-ray intensity by 50% from its initial value. Moreover, the μ is also used in the calculation of TVL. The TVL was obtained from $TVL = 2.303/\mu$, which represents the thickness of the interacting medium required to attenuate a radiation beam to 10% of its initial level. In addition, the theoretical values of mass attenuation coefficients (MAC, μ_m) of the samples can be defined as a compound rule [25]: $\mu_m = \sum_i w_i(\mu_m)_i$, where w_i is the weight fraction of each element in the sample. The MAC_{xcom} values of the PVA/PVP: MO blend films can be calculated for selected energy using the XCOM program [22, 23].

RESULTS AND DISCUSSION

Transmission behavior in the presence of primary ionizing radiation is a significant aspect of the evaluation

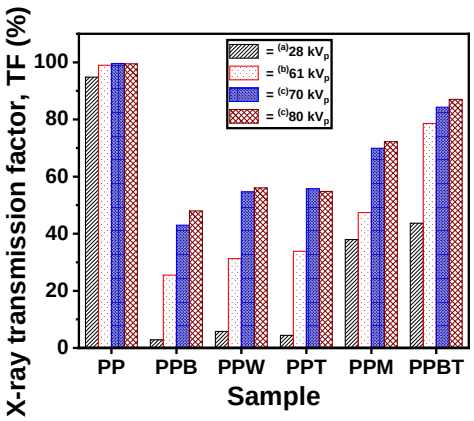

Fig. 3 The TF of the PVA/PVP: MO blend films evaluated at the following X-ray tube voltages: (a) 28 kV_p for a mammogram X-ray machine, (b) 61 kV_p for an intraoral X-ray machine, and (c) 70 and 80 kV_p for a general X-ray machine.

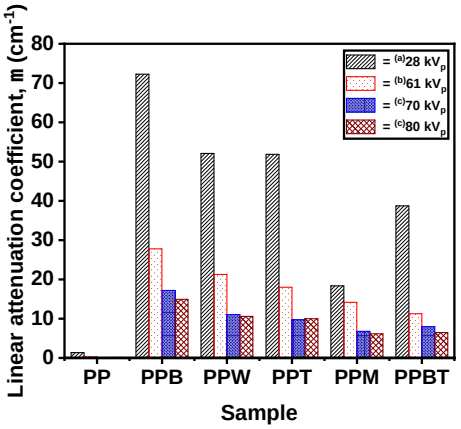

Fig. 4 The LAC of the PVA/PVP: MO blend films measured at the following X-ray tube voltages: (a) 28 kV_p for a mammogram X-ray machine, (b) 61 kV_p for an intraoral X-ray machine, and (c) 70 and 80 kV_p for a general X-ray machine.

of materials intended for use in radiation fields. In this study, the TF values of the PVA/PVP: MO blend films were measured at various X-ray tube voltages, and the results were shown in Fig. 3. The result showed that the TF was decreased by the increment of tube voltage. The PVA/PVP composite filled with 50 wt% Bi_2O_3 (PPB) with a thickness of 0.49 mm exhibited a greater shielding ability than other high-Z compounds, such as WO_3, Ta_2O_5, MoO_3, and $BaTiO_3$. The TF of the PPB sample was found to be 2.87% for a mammogram at 28 kV_p and 25.51% for an intraoral X-ray machine at 61 kV_p. The TF was 42.99% at 70 kV_p and 47.99% at 80 kV_p using a general X-ray machine. In comparison to other studies on low-energy X-rays, the TF values of the PPB (0.49 mm thick), PPW (0.55 mm thick), and PPT (0.60 mm thick) samples were observed to be nearly equal to that of the PVA film doped with 18 wt% Bi_2O_3-NPs (0.25 mm thick), which exhibited a TF of less than 2% at 25–35 kV_p [19]. Additionally, the TF of the PVC matrix containing 50 wt% Bi_2O_3 (1 mm thick) was 3% at 20–30 kV_p and 27% at 61 kV_p [26]. For high-energy X-ray (at 80 kV_p), the PVA/PVP: MO samples showed lower TF values than 65 wt% $Bi_4Ti_3O_{12}$ loaded epoxy composites (TF = 14.90%, 1.52 mm thick) [9], the PVP-PEG matrix doped with 50 wt% Bi_2O_3-$BaTiO_3$ nanocomposites (TF = 25%, 1.42 mm thick) [10], 44.44 wt% Bi_2O_3 loaded PDMS (TF = 25%, 1.23 mm thick) [27], and the PS sample filled with 66.67 wt% of Bi_2O_3 (TF = 8%, 1.33 mm thick) [28]. However, the TF of the PVA/PVP composites filled with MOs could be further improved by adjusting the concentration of co-dopants [14] and high-Z metals [15], incorporation of nanoparticles [14, 15], and/or modifying the film thickness [29]. In addition, the obtained attenuation performance suggested that the developed thin PVA/PVP-based composite films were potentially suitable for use in radiation attenuating protective gloves (TF < 78% at 80 kV_p), in compliance with the requirements of ASTM International D7866 [30].

The LAC represents the fraction of the incident photon beam that is absorbed or scattered per unit length within a material. Variations in the LAC values as a function of kV_p are illustrated in Fig. 4. The sample with 50 wt% Bi_2O_3 loading exhibited the highest LAC value compared to the other samples. The LAC of the PPB sample was reported to be 72.28 cm^{-1} at 28 kV_p using mammography, 27.80 cm^{-1} at 61 kV_p with an intraoral X-ray machine, and 17.17 cm^{-1} and 14.94 cm^{-1} at 70 kV_p and 80 kV_p using a general X-ray machine, respectively. Based on the experimental data, 50 wt% MoO_3 loaded PVA/PVP composites demonstrated the lowest LAC among the samples with different filler loadings at 28, 70, and 80 kV_p due to its lowest atomic number. Additionally, at 61 kV_p, the sample with 50 wt% $BaTiO_3$ loading showed the lowest LAC values. The dental X-ray tube operated at around 60 kV_p, corresponding to mean energies of approximately 34 to 39 keV [3–5], at which the photoelectric absorption at L-, M-, and K-edge of Ba and Ti exhibited the lowest absorption ability within this range. The K-edge effect involved a sudden increase in the X-ray attenuation coefficient attributed to the highest photoelectric absorption of photons occurring at a specific photon energy just above the binding energy of the K-shell electron of the metal atoms that interact with the photons. The K-edge values of Mo, Ba, Ti, Ta, W, and Bi were reported to be 20.0, 37.4, 49.6, 67.4, 69.5, and 90.5 keV, respectively [21]. The photoelectric effect is generally the predominant mechanism of photon interaction at lower photon energies and higher Z numbers, due to

Table 1 Comparison of LAC values reported in previous studies on polymer composites with high-Z materials.

Base material	Filler	LAC (cm^{-1})	Reference
PVA/PVP	50 wt% Bi_2O_3	14.94 cm^{-1}@80 kV_p	This work
	50 wt% WO_3	10.60 cm^{-1}@80 kV_p	
	50 wt% Ta_2O_5	9.99 cm^{-1}@80 kV_p	
	50 wt% MoO_3	6.18 cm^{-1}@80 kV_p	
	50 wt% $BaTiO_3$	6.47 cm^{-1}@80 kV_p	
Epoxy	50 wt% Pb_3O_4	30.91 cm^{-1}@29 kV_p	Yahya KW, et al [14]
	50 wt% Pb_3O_4+Fe_2O_3	26.94 cm^{-1}@29 kV_p	
	50 wt% $BaSO_4$	14.57 cm^{-1}@29 kV_p	
Polylactic acid (PLA)	38 wt% Bi_2O_3-NPs	74.43 cm^{-1}@30 kV_p	Noor Azman NZ, et al [31]
	38 wt% Bi_2O_3	67.34 cm^{-1}@30 kV_p	
Polyvinyl Chloride (PVC)	50 wt% Ta_2O_5-NPs	12.73 cm^{-1}@70 kV_p	Nuñez-Briones AG, et al [14]
	50 wt% Bi_2O_3-NPs	17.81 cm^{-1}@70 kV_p	
	50 wt% Ta_2O_5+Bi_2O_3-NPs	19.15 cm^{-1}@70 kV_p	
PVA/PVP	24 wt% WO_3	4.68 cm^{-1}@60 kV_p	Bijanu A, et al [17]
		4.27 cm^{-1}@70 kV_p	
		4.12 cm^{-1}@80 kV_p	
PVA/PVP	26.27 wt% Bi_2O_3	11.84 cm^{-1}@60 kV_p	Bijanu A, et al [18]
		10.05 cm^{-1}@70 kV_p	
Epoxy	20 wt% Pb	2.52 cm^{-1}@80 kV_p	Omidtorshiz A, et al [32]
	20 wt% PbO	2.72 cm^{-1}@80 kV_p	
	20 wt% PbO-NPs	3.54 cm^{-1}@80 kV_p	
Polystyrene (PS)	35 wt% PbO-NPs	1.88 cm^{-1}@80 kV_p	Osman AF, et al [33]
Waterborne polyurethane	60 wt% Bi_2O_3	11.53 cm^{-1}@80 kV_p	Koyuncu B, et al [34]
Epoxy	50 wt% PbO	12.53 cm^{-1}@80 kV_p	Azman NZN, et al [35]
	50 wt% Pb_3O_4	12.22 cm^{-1}@80 kV_p	

its dependence on the $(Z/E)^3$ scaling [16, 31]. During this interaction, a photon is completely absorbed by the atoms of the material, resulting in the ejection of a photoelectron. The ejected photoelectron may undergo subsequent interactions with neighboring atoms. Furthermore, Compton scattering can occur between the incident photon and an outer-shell electron of an atom within the absorbing material. Compton scattering probability is nearly independent of X-ray energy and atomic number. In contrast, the probability of the photoelectric effect decreases significantly with increasing photon energy, resulting in Compton scattering becoming the dominant interaction mechanism at higher X-ray energies. The LAC values reported in previous studies on various polymer composites with high-Z materials were showed in Table 1. Compared to other samples, the LAC values of the PPB, PPW, and PPT composites were higher than those of the PLA composites containing 38 wt% Bi_2O_3-NPs and Bi_2O_3 [31] as well as epoxy composites filled with 50 wt% of PbO_3O_4, PbO_3O_4+Fe_2O_3, and $BaSO_4$ [12] at low energy X-rays ($\leqslant$30 kV_p). In addition, the LAC values of the PPW and PPB samples were higher than those of the PVA/PVP matrix doped with 24 wt% WO_3 and 26.27 wt% Bi_2O_3 loaded PVA/PVP composites [17, 18]. This difference of LAC values could be attributed to the varying concentration of high-Z metals. At 70 kV_p, the LAC of the PPB sample was nearly equal to that of PVC loaded with 50 wt% Bi_2O_3-NPs and higher than that of the PVC mixed with 50 wt% Ta_2O_5-NPs [14]. At 80 kV_p, the LAC of the PVA/PVP samples loaded with Bi_2O_3, WO_3, Ta_2O_5, MoO_3, and $BaTiO_3$ were significantly higher than those of other polymers filled with $\leqslant$35 wt% of PbO-NPs, Pb, and PbO [32, 33]. Specifically, the LAC of the PPB sample was higher than that of waterborne polyurethane containing 60 wt% of Bi_2O_3 [34] and epoxy composites filled with 50 wt% of PbO and Pb_3O_4 [35]. Therefore, 50 wt% Bi_2O_3 loaded PVA/PVP composites could serve as a suitable alternative to Pb-based compounds in X-ray shielding materials.

As shown in Table 2, the HVL and TVL of the PVA/PVP: MO composite films increased with increasing kV_p, indicating that higher radiation energies enhance photon penetration through the material. These results demonstrated that lower energy photons require thinner shielding materials for effective attenuation, whereas higher energy photons necessitate increased material thickness to achieve comparable attenuation levels. The lowest HVL and TVL corre-

Table 2 The HVL and TVL of the PVA/PVP: MO blend films.

Sample	HVL (cm)				TVL (cm)			
	[(a)] 28 kV_p	[(b)] 61 kV_p	[(c)] 70 kV_p	[(c)] 90 kV_p	[(a)] 28 kV_p	[(b)] 61 kV_p	[(c)] 70 kV_p	[(c)] 90 kV_p
PP	0.517	2.730	6.636	5.453	1.718	9.068	22.045	18.113
PPB	0.010	0.025	0.040	0.046	0.032	0.083	0.134	0.154
PPW	0.013	0.033	0.063	0.065	0.044	0.108	0.208	0.217
PPT	0.013	0.038	0.071	0.069	0.044	0.128	0.237	0.230
PPM	0.038	0.049	0.102	0.112	0.125	0.163	0.340	0.373
PPBT	0.018	0.062	0.087	0.107	0.059	0.204	0.289	0.356

(a) mammogram X-ray machine operated at 28 kV_p, (b) intraoral X-ray machine operated at 61 kV_p, and (c) general X-ray machine operated at 70 and 80 kV_p.

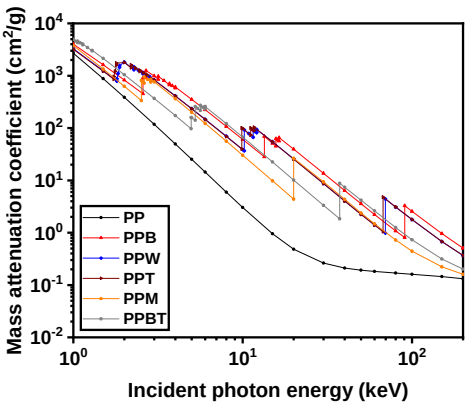

Fig. 5 The MAC_{xcom} of the PVA/PVP: MO blend films in a wide energy range from 1 keV to 200 keV using the XCOM program.

sponded to the superior attenuation performance of the PVA/PVP: MO composite films. Among the tested samples, the PPB sample exhibited the lowest HVL and TVL values at 28 kV_p (mammography unit), 61 kV_p (intraoral X-ray machine), and within the 70–80 kV_p range (general X-ray machine). However, the results of HVL and TVL indicate the potential of these composites to contribute to safer medical diagnostic environments, particularly through the use of appropriately thickened shields tailored to specific energy ranges.

In the present work, the XCOM-calculated MAC values were employed as theoretical references to understand the intrinsic photon–matter interaction mechanisms of the composite materials over the relevant diagnostic energy range. To relate the monoenergetic data to the experimental conditions, the comparison was conducted within the reported mean photon energy ranges corresponding to each tube voltage (e.g., ~20 keV at 28 kV_p [2], 34–39 keV at 60 kV_p [3–5], and 39–46 keV at 70–80 kV_p [3–5]). Since the diagnostic X-ray beams were inherently polychromatic, the use of mean photon energy provided an appropriate approximation for correlating the theoretically calculated attenuation coefficients. The mass attenuation coefficients (MAC_{xcom}) of the PVA/PVP composites filled with MOs were calculated using the XCOM program [22, 23] as illustrated in Fig. 5. The XCOM results showed a consistent decrease in MAC_{xcom} values with increasing photon energy. In contrast, the incorporation of metal oxides into the PVA/PVP matrix enhanced MAC_{xcom} values, particularly near the K-, L-, and M-shell absorption edges. For example, the absorption edges for various elements were reported [21] as follows: for Bi, the edges at K, L1, L2, L3, M1, and M5 were 90.5, 16.4, 15.7, 13.4, 4.0, and 2.6 keV, respectively. For W, the absorption edges were 69.5, 12.1, 11.5, 10.2, 2.8, and 1.8 keV. Similarly, for Ta, the edges were 67.4, 11.7, 11.1, 9.9, 2.7, and 1.7 keV, respectively. These results demonstrated that each dopant enhanced photon attenuation within specific energy regions. The Bi contributed more effectively near higher absorption edge energies, whereas W and Ta provided stronger attenuation at relatively lower energies. This complementary behavior explained the enhanced radiation attenuation performance observed in composites incorporated with multiple metal oxide dopants. For example, the MAC of the Ta_2O_5–Bi_2O_3/PVC composite was reported to be higher than those of lead, Ta_2O_5/PVC, and Bi_2O_3/PVC composites [14]. In this study, within the mean energy range of 20 to 50 keV, the PPB composite demonstrated the highest MAC, with values of 40.47, 14.30, 6.84, and 3.87 cm^2/g at photon energies of 20, 30, 40, and 50 keV, respectively.

Previous studies have demonstrated that the tensile strength of PVA and PVP/PVA composite systems may increase with increasing incorporation of metal oxides such as Bi_2O_3, WO_3, MoO_3, and $BaTiO_3$ [36–39]. This improvement has been attributed to enhanced interfacial interactions between filler particles and polymer chains. Considering their attenuation performance, the developed thin PVA/PVP-based composite films are potentially suitable for application such as radiation-attenuating protective gloves [30]. Owing to its superior TF, LAC, and MAC_{xcom} values, together with the lowest observed HVL and TVL, the PPB composite exhibits strong potential as aviable

alternative to conventional lead-based materials for X-ray shielding applications.

CONCLUSION

PVA/PVP blend films containing 50 wt% MOs, including Bi_2O_3, WO_3, Ta_2O_5, MoO_3, and $BaTiO_3$, were successfully fabricated using the solution casting technique. The shielding properties of these composites were evaluated based on TF, LAC, HVL, and TVL. The results showed that the PVA/PVP composite loaded with 50 wt% Bi_2O_3 at a thickness of 0.49 mm exhibited the lowest TF and the highest LAC compared to the other metal oxides. The X-attenuation ability was influenced by both the energy of the incident photons and the atomic number of the incorporated metal oxide. Furthermore, the PPB sample showed the lowest HVL and TVL, indicating superior shielding performance. The XCOM data revealed that the PPB sample exhibited the highest MAC_{xcom} within the photon energy range of 20–50 keV, corresponding to the mean energy of the X-ray tube used in this study. All results indicated that the developed PVA/PVP blend films containing 50 wt% Bi_2O_3 exhibited greater X-ray attenuation compared to other metal oxides. Beyond its shielding efficiency, the PPB composite offers significant advantages in terms of environmental safety and ease of fabrication, addressing the inherent limitations of traditional lead-based shielding materials. The integration of non-toxic, lightweight materials into medical protective equipment holds the potential to contribute substantially to safer environments, ensuring both improved patient safety and reduced environmental impact.

Acknowledgements: This research was supported by the Fundamental Fund (FF2568) of Rajamangala University of Technology Lanna, Chiang Mai, Thailand. Additionally, the Regional Medical Sciences Center 1 in Chiang Mai assisted with the X-ray attenuation measurements, and the Department of Physics and Materials Science, Faculty of Science, Chiang Mai University, Thailand provided support for the preparation process.

REFERENCES

1. Jayakumar S, Saravanan T, Philip J (2023) A review on polymer nanocomposites as lead-free materials for diagnostic X-ray shielding: Recent advances, challenges and future perspectives. *Hybrid Adv* **4**, 100100.
2. Williams MB, Simoni PU, Smilowitz L, Stanton M, Phillips W, Stewart A (1999) Analysis of the detective quantum efficiency of a developmental detector for digital mammography. *Med Phys* **26**, 2273–2285.
3. Santos MAP, Fragoso MCF, Lima RA, Hazin CA (2009) X-ray beam qualities for dental radiology purposes. In: *Proceedings of the International Nuclear Atlantic Conference (INAC 2009)*, Rio de Janeiro, Brazil.
4. Poirie Y, Kuznetsova S, Villarreal-Barajas JE (2018) Characterization of nanoDot optically stimulated luminescence detectors and high-sensitivity MCP-N thermoluminescent detectors in the 40–300 kV_p energy range. *Med Phys* **45**, 402–413.
5. McCaffrey JP, Shen H, Downton B, Mainegra-Hing E (2007) Radiation attenuation by lead and nonlead materials used in radiation shielding garments. *Med Phys* **34**, 530–537.
6. Carroll QB (2023) *Radiography in the Digital Age: Physics–Exposure–Radiation Biology*, Charles C Thomas Publisher, Illinois, USA.
7. Mizumatsu S, Monje ML, Morhardt DR, Rola R, Palmer TD, Fike JR (2003) Extreme sensitivity of adult neurogenesis to low doses of X-irradiation. *Cancer Res* **63**, 4021–4027.
8. Bawazeer O, Albakri H, Makkawi K, Aga ZB, Alomari A, Adil SF, Algethami M, Assiri N, et al (2025) Evaluation of X-ray shielding performance of Bi/PMMA and Bi/PMMA–TiO_2/PMMA nanocomposites. *Radiat Phys Chem* **231**, 112596.
9. Yu L, Yap PL, Santos A, Tran D, Losic D (2021) Lightweight bismuth titanate ($Bi_4Ti_3O_{12}$) nanoparticle-epoxy composite for advanced lead-free X-ray radiation shielding. *ACS Appl Nano Mater* **4**, 7471–7478.
10. Bawazeer O, Baatiyah B, Al Amoudi S, Aga Z, Matar Z, Khan S, Al-Qahtani S, Algethami M, et al (2025) Evaluation of X-ray radiation shielding performance of Bi_2O_3 and $BaTiO_3$ embedded in PVP and PEG polymer nanocomposite. *Radiat Eff Defects Solids* **180**, 463–475.
11. El Rahman A, Metwally HS, Sabry N, Mohammed MI (2024) Gamma-ray shielding effectiveness, optical, mechanical, dielectric properties of nanofiller-reinforced PVA/PVP polymeric blend nanocomposites. *Sci Rep* **14**, 27466.
12. Yahya KW, Khadeer EE (2021) Study the effect of weight fractions of different powders on the attenuation performances of the epoxy composite. *NeuroQuantology* **19**, 142–151.
13. Sanjeevi P, Varuna J, Puviarasu P, Alothman AA, Ramadan R, Sangaraju S, Elango M (2025) Study on super mitigating and synergistic properties of MoO_3 and Mg:MoO_3 impregnated epoxy resin nanocomposite for the development of X-ray shielding aprons. *Radiat Phys Chem* **232**, 112656.
14. Nuñez-Briones AG, Benavides R, Bolaina-Lorenzo ED, Martínez-Pardo ME, Kotzian-Pereira-Benavides C, Mendoza-Mendoza E, Bentacourt-Galindo R, Garcia-Cerda LA (2023) Nontoxic flexible PVC nanocomposites with Ta_2O_5 and Bi_2O_3 nanoparticles for shielding diagnostic X-rays. *Radiat Phys Chem* **202**, 110512.
15. Shik NA, Gholamzadeh L (2018) X-ray shielding performance of the EPVC composites with micro- or nanoparticles of WO_3, PbO or Bi_2O_3. *Appl Radiat Isot* **139**, 61–65.
16. Kamaruddin KE, Kok SY, Ramli RM, Azman NZN (2024) X-ray attenuation measurement of electrospun polymer composite mats containing Bi_2O_3/WO_3 nanofillers as X-ray shielding material. *Appl Phys A* **130**, 455.
17. Bijanu A, Paulose R, Tomar AS, Agrawal V, Gowri VS, Sanghi SK, Khan R, Khan MA, et al (2022) Chemically bonded tungsten-based polymer composite for X-rays shielding applications. *Mater Today Commun* **32**, 104100.
18. Bijanu A, Rajak G, Paulose R, Arya R, Agrawal V, Gowri VS, Khan MA, Salammal ST, et al (2023) Flexible, chemically bonded Bi-PVA–PVP composite for enhanced diagnostic X-ray shielding applications. *J Inorg Organomet Polym* **33**, 2279–2291.

19. Noor Azman NZ, Musa NFL, Nik Ab Razak NNA, Ramli RM, Mustafa IS, Rahman AA, Yahaya NZ (2016) Effect of Bi_2O_3 particle sizes and addition of starch into Bi_2O_3–PVA composites for X-ray shielding. *Appl Phys A* **122**, 818.
20. Phattarateera S, Xin L, Kaewpheng K, Kriangburananan T, Threepopnatkul P (2023) Effects of additives on properties of PVA film for agricultural applications. *ScienceAsia* **49S**, 23–31.
21. Bearden JA, Burr AF (1967) Reevaluation of X-ray atomic energy levels. *Rev Mod Phys* **39**, 125–142.
22. Gerward L, Guilbert N, Jensen KB, Levring H (2001) X-ray absorption in matter: Reengineering XCOM. *Radiat Phys Chem* **60**, 23–24.
23. Gerward L, Guilbert N, Jensen KB, Levring H (2004) WinXCom: A program for calculating X-ray attenuation coefficients. *Radiat Phys Chem* **71**, 653–654.
24. International Electrotechnical Commission (2014) Protective devices against diagnostic medical X-radiation – Part 1: Determination of attenuation properties of materials. *IEC*, 61331-1.
25. Jackson DF, Hawkes DJ (1981) X-ray attenuation coefficients of elements and mixtures. *Phys Rep* **70**, 169–233.
26. Nuñez-Briones AG, Benavides R, Mendoza-Mendoza E, Martínez-Pardo ME, Carrasco-Abrego H, Kotzian C, Saucedo-Zendejo FR, García-Cerda LA (2021) Preparation of PVC/Bi_2O_3 composites and their evaluation as low energy X-Ray radiation shielding. *Radiat Phys Chem* **179**, 109198.
27. Nambiar S, Osei EK, Yeow JTW (2012) Polymer nanocomposite-based shielding against diagnostic X-rays. *J Appl Polym Sci* **127**, 4939–4946.
28. Maghrabi HA, Vijayan A, Deb P, Wang L (2015) Bismuth oxide-coated fabrics for X-ray shielding. *Text Res J* **86**, 649–658.
29. Shueb MI, Omar RS, Umar KNK, Bakar AAA, Karim J, Esa F, Sapuan SZ, Khee YS, et al (2026) Lead-free HDPE nanocomposites for multifunctional neutron–gamma–electromagnetic interference shielding. *Radiat Phys Chem* **241**, 113494.
30. ASTM (2023) *ASTM D7866-23: Standard Specification for Radiation Attenuating Protective Gloves*. ASTM International, West Conshohocken, PA, USA.
31. Noor Azman NZ, Siddiqui SA, Haroosh HJ, Albetran HM, Johannessen B, Dong Y, Low IM (2013) Characteristics of X-ray attenuation in electrospun bismuth oxide/polylactic acid nanofibre mats. *J Synchrotron Radiat* **20**, 741–748.
32. Omidtorshiz A, Benam MR, Momennezhad M, Sabouri Z, Darroudi M (2025) Shielding characteristics of a new epoxy resin reinforced by PbO nanoparticles and PbO micro for protection against X-ray and investigation of their cytotoxicity effects and photocatalytic activity. *Radiat Phys Chem* **226**, 112324.
33. Osman AF, Balaa HEI, Samad OEI, Awad R, Badawi MS (2023) Assessment of X-ray shielding properties of polystyrene incorporated with different nano sizes of PbO. *Radiat Environ Biophys* **62**, 235–251.
34. Koyuncu B, Aral N, Candan C, Nergis B (2024) Bismuth oxide nanoparticles/waterborne polyurethane-coated fabrics for ionizing radiation protection. *J Coat Technol Res* **21**, 969–978.
35. Azman NZN, Siddiqui SA, Hart R, Low IM (2013) Microstructural design of lead oxide–epoxy composites for radiation shielding purposes. *J Appl Polym Sci* **128**, 3213–3219.
36. Tiamduangtawan P, Kamkaew C, Kuntonwatchara S, Wimolmala E, Saenboonruang K (2023) Comparative mechanical, self-healing, and gamma attenuation properties of PVA hydrogels containing either nano- or micro-sized Bi_2O_3 for use as gamma-shielding materials. *Radiat Phys Chem* **177**, 109164.
37. Rithin Kumar NB, Crasta V, Praveen BM (2015) Enhancement of optical, mechanical and micro structural properties in nanocomposite films of PVA doped with WO_3 nanoparticles. *Int J Struct Integr* **6**, 338–354.
38. Rajesh K, Crasta V, Rithin Kumar NB, Shetty G, Sangappa Y, Kudva J, Vijeth H (2019) Effect of MoO_3 nanofiller on structural, optical, mechanical, dielectric and thermal properties of PVA/PVP blend. *Mater Res Innovations* **24**, 270–278.
39. Shareef NM, Madhuri W (2023) Structural, morphological, dielectric and tensile properties of $BaTiO_3$ doped PVA/PVP polymer blend nanocomposites. *Polym Bull* **80**, 2389–2412.